

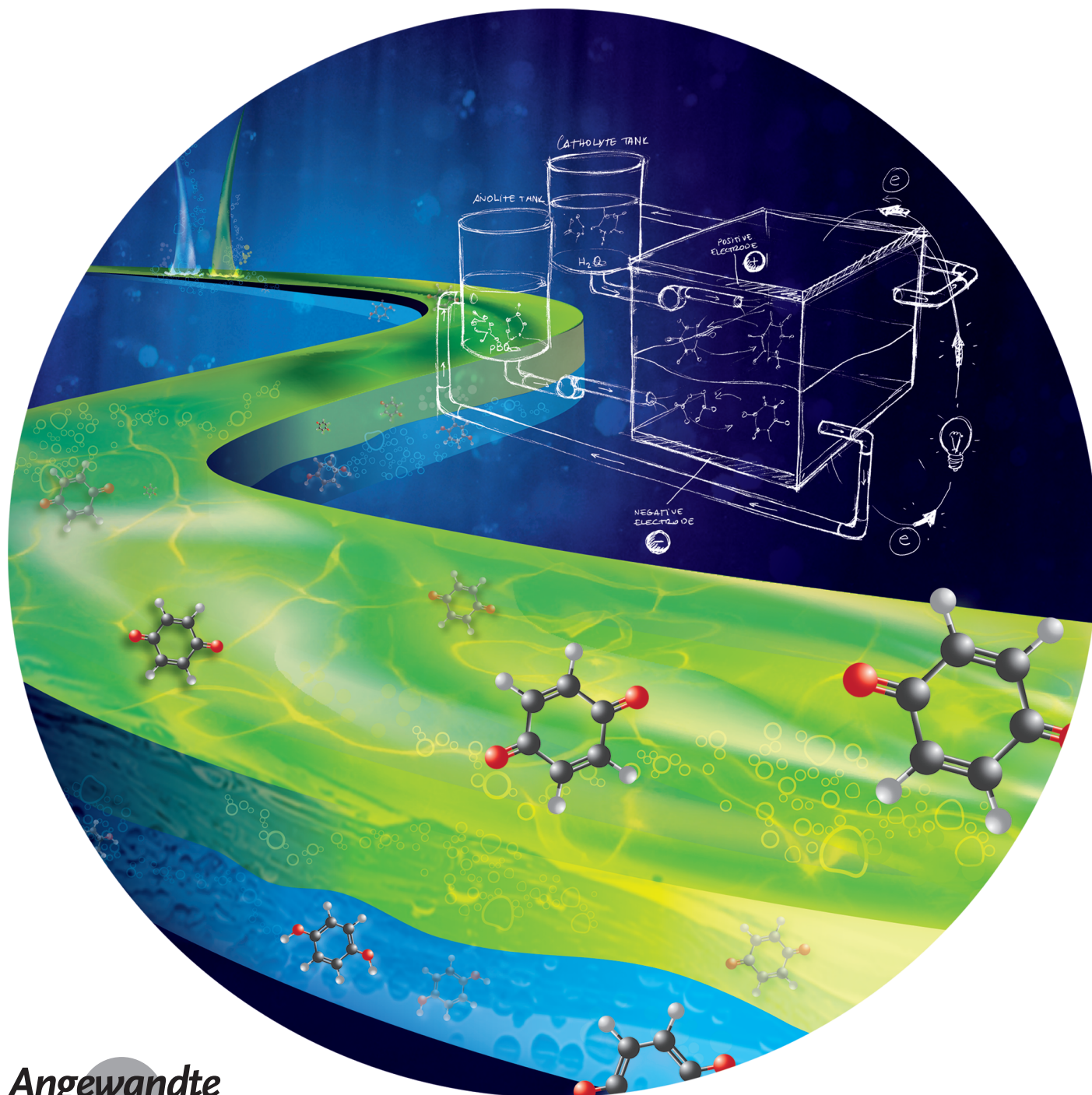
Batteries

International Edition: DOI: 10.1002/anie.201704318

German Edition: DOI: 10.1002/ange.201704318

A Membrane-Free Redox Flow Battery with Two Immiscible Redox Electrolytes

Paula Navalpotro, Jesus Palma, Marc Anderson, and Rebeca Marcilla*



Angewandte
International Edition
Chemie

Abstract: Flexible and scalable energy storage solutions are necessary for mitigating fluctuations of renewable energy sources. The main advantage of redox flow batteries is their ability to decouple power and energy. However, they present some limitations including poor performance, short-lifetimes, and expensive ion-selective membranes as well as high price, toxicity, and scarcity of vanadium compounds. We report a membrane-free battery that relies on the immiscibility of redox electrolytes and where vanadium is replaced by organic molecules. We show that the biphasic system formed by one acidic solution and one ionic liquid, both containing quinoyl species, behaves as a reversible battery without any membrane. This proof-of-concept of a membrane-free battery has an open circuit voltage of 1.4 V with a high theoretical energy density of 22.5 Wh L⁻¹, and is able to deliver 90% of its theoretical capacity while showing excellent long-term performance (coulombic efficiency of 100% and energy efficiency of 70%).

The development of energy-storage technologies capable of fulfilling the needs of renewable energy sources has become one of the most critical challenges of this century. Indeed, flexible and scalable energy-storage solutions are necessary for alleviating intermittent fluctuations in renewable-energy sources allowing their massive incorporation to the grid^[1] and diminishing our undesired fossil fuel dependency.^[2] Differing from conventional batteries, redox flow batteries (RFBs) utilize electroactive species that are dissolved in the electrolytes and stored in two external tanks, making it possible to decouple power and energy.^[3,4] This approach constitutes a significant advantage when large batteries have to be accurately dimensioned. The most developed RFB technology involves the aqueous All-Vanadium system, discovered in the 1980s,^[5] whose major issues are the low performance, short lifetime, and high cost of the ion-selective membranes and the high price, toxicity, and scarcity of vanadium compounds.^[6] After a long period without significant progress, RFBs have recently experienced rejuvenated interest mainly triggered by the penetration of renewable energies into the energy market.^[6] One of the most promising research topics has been the replacement of the problematic vanadium compounds by organic redox molecules that are abundant, low cost, and environmental friendly.^[7] Some pioneering examples include organic RFBs based on quinoid-type redox

couples in acid^[8] and alkaline electrolytes.^[9] Another encouraging research line is the substitution of aqueous electrolytes by non-aqueous electrolytes^[10] or even ionic liquids,^[11] which are more electrochemically stable and would allow achieving higher battery voltages and energy densities.^[12,13] In the last few years, RFBs based on organic redox molecules, such as quinones, phenothiazine, nitroxides, viologens, and pyridines^[14-17] have experienced a great deal of interest, becoming one of the hottest topics in electrochemical energy storage (see Table S1 in the Supporting Information).^[18,19] Regardless of the chemical nature of the electroactive species and the type of electrolytes, most RFBs rely on ion-selective membranes to separate the two redox electrolytes and to prevent the crossover of active compounds while allowing the migration of charge carriers. It is worth mentioning that membranes are not employed in some hybrid RFBs in which one of the active species is a solid, such as Zn,^[20,21] Cd,^[22] lithium,^[23] or graphite.^[24] However, in this hybrid RFB technology is not possible to fully decouple power and energy, this decoupling however is probably the most important advantage of redox flow batteries over conventional ones. Therefore, ion-selective membranes still remain one of the obstacles for the massive commercialization of RFBs because they are expensive (approaching 40% of the total cost)^[25] and limit the performance and lifetimes of RFBs.^[26,27] The polymer-based system introduced a novel principle of separating the cathode and anode by size-exclusion^[28] but the only way to completely eliminate membranes in RFBs so far has been through the development of fluidodynamic engineering solutions to maintain a laminar flow minimizing the mixture of the electrolytes.^[29-32] Most of these batteries exploit the laminar flow of electrolytes through parallel micro-channels and thus their real applications are limited to power small micro-devices.

As a new direction in battery philosophy, we propose a membrane-free redox flow battery based on the use of immiscible electrolytes that spontaneously form a biphasic system whose interphase functions as a “natural” barrier making a membrane superfluous. A schematic representation of this membrane-free concept is shown in Figure 1. Different from the laminar-flow strategy, this membrane-free concept is feasible to scale-up and highly versatile since it does not depend on the flux regime and can be applied to different types of aqueous and non-aqueous immiscible electrolytes. Contrary to hybrid RFBs, in our membrane-free battery both active species are liquid electrolytes so that power and energy are totally decoupled. Specifically, we demonstrate that an acidic solution of hydroquinone (H₂Q) and a hydrophobic ionic liquid (IL), 1-butyl-1-methylpyrrolidinium bis(trifluoromethanesulfonyl)imide (PYR₁₄TFSI) containing dissolved parabenzoquinone (pBQ), spontaneously forms a liquid-liquid biphasic system that perfectly behaves as a battery without the need of any membrane or physical separator. The choice of pBQ and H₂Q as redox-active organic molecules is motivated by their simplicity, relatively high solubility in the electrolytes (ca. 0.7 M for aqueous and IL electrolyte) and their theoretical capacity; 495 mAhg⁻¹ and 486 mAhg⁻¹ for pBQ and H₂Q, respectively. It is remarkable that, by taking advantage of the different redox mechanism underwent by

[*] P. Navalpotro, Dr. J. Palma, Prof. M. Anderson, Dr. R. Marcilla
Electrochemical Processes Unit, IMDEA Energy Institute
Avda. Ramón de la Sagra 3, 28935 Móstoles (Spain)
E-mail: rebecca.marcilla@imdea.org

Prof. M. Anderson
Department of Civil and Environmental Engineering
University of Wisconsin
Madison, WI 53706 (USA)

Supporting information and the ORCID identification number(s) for the author(s) of this article can be found under:
<https://doi.org/10.1002/anie.201704318>.

© 2017 The Authors. Published by Wiley-VCH Verlag GmbH & Co. KGaA. This is an open access article under the terms of the Creative Commons Attribution Non-Commercial License, which permits use, distribution and reproduction in any medium, provided the original work is properly cited, and is not used for commercial purposes.

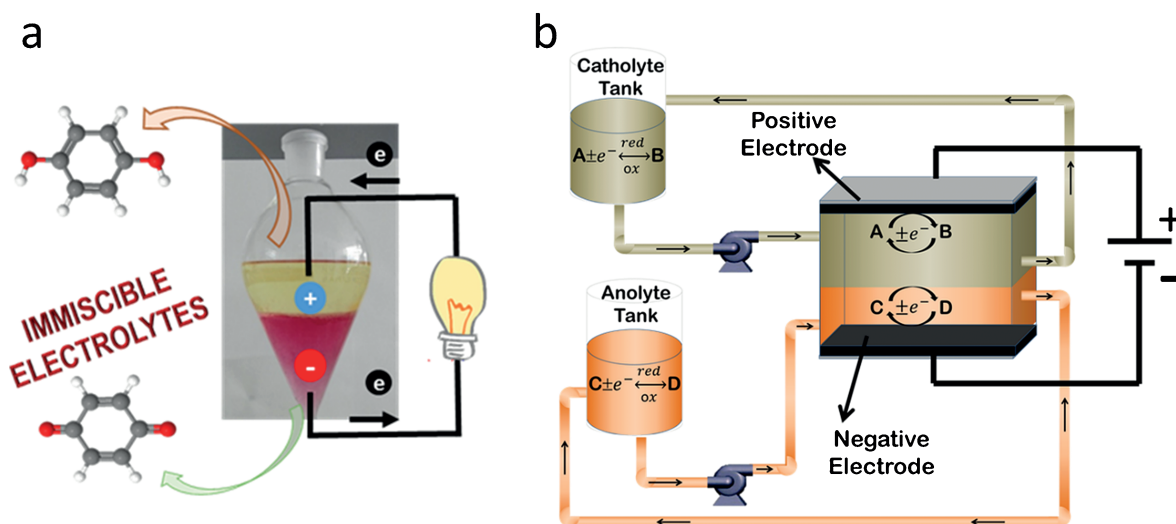


Figure 1. a) Schematic representation of the membrane-free battery concept based on immiscible redox electrolytes where the upper phase is the aqueous electrolyte that acts as the catholyte and the lower phase is the ionic liquid electrolyte which is the anolyte. b) Membrane-free flow battery with a horizontal design to favor the formation of the two immiscible phases.

quinones in different electrolytes, the same molecule was used as active species in both electrolytes. Moreover, similar to all-vanadium RFB technology, in this particular example pBQ and H₂Q constitute different oxidation states of the same molecule meaning that the eventual cross-over would provoke certain loss of efficiency but not irreversible contamination. Finally, both compounds have a low molecular weight-to-charge ratio of 54 g/(mol e⁻) and 55 g/(mol e⁻), respectively. This is substantially less than 150 g/(mol e⁻) proposed by Sandford and co-workers for achieving grid-cost parity.^[33]

The immiscible catholyte and anolyte forming the biphasic system (acidic solution of hydroquinone (H₂Q) and parabenzoquinone (pBQ) dissolved in PYR₁₄TFSI) were subjected to cyclic voltammetry (CV) in 3-electrode electrochemical cells, separately. The shape of the CVs in Figure 2 denotes a quasi-reversible redox behavior for both electrolytes. As reported elsewhere, hydroquinone (H₂Q) in acidic media suffers a reversible oxidation to parabenzoquinone

(pBQ) in one step, involving the exchange of 2 electrons and 2 protons.^[34] On the other hand, the parabenzoquinone (pBQ) in aprotic electrolyte undergoes a two consecutive reversible reduction reactions to radical anion (pBQ^{-•}) and dianion (pBQ^{2-•}), exchanging 2 electrons in total.^[35] It should be highlighted that, the same simple molecule follow different redox reaction pathways occurring at different redox potentials, depending on the protic/aprotic nature of the electrolyte. Although this has been reported before, this is the first time in which this voltage difference is exploited to develop a symmetric battery. This “symmetric design” offers advantages such as mitigating chemical contamination associated with crossover of the electrolytes. Until now, these benefits have been limited to complex redox molecules having multiple oxidation states^[36–38] but with the development of this membrane-free concept the opportunities boost greatly. The position of potentials in the CVs in Figure 2 anticipates an open circuit voltage (OCV) of about 1.4 V for the battery assembled by combining these two immiscible electrolytes. This OCV is higher than previous examples of RFBs based on quinoyl species.^[8,9,39] This is likely due to the ionic liquid, which is electrochemically more stable than former aqueous electrolytes and allows the reduction of pBQ at more negative voltages. The redox mechanisms described above and represented in Figure 2b,c were confirmed by rotating disk electrode (RDE) experiments that were used to calculate the diffusion coefficients and rate constants for both redox electrolytes (see Figure S1 in the Supporting Information). As expected, the lower conductivity and higher viscosity of the ionic liquid electrolyte (2.2 mS cm⁻¹ and 84.33 cP in comparison with 392 mS cm⁻¹ and 0.92 cP for aqueous electrolyte)^[40] leads to more

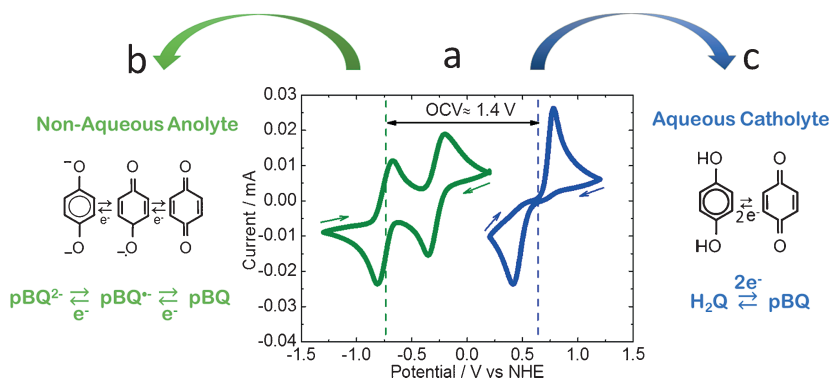


Figure 2. Electrochemical characterization of immiscible redox electrolytes. a) Cyclic voltammetry experiments of 20 mM pBQ in PYR₁₄TFSI (green) and 20 mM H₂Q in 0.1 M HCl (blue) performed in 3-electrode electrochemical cells (scan rate = 10 mV s⁻¹) b),c) Redox-active organic species in both electrolytes and their corresponding redox mechanisms depending on the nature of the electrolyte.

significant mass transport and kinetic limitations that are evidenced by the lower diffusion coefficient (D) and rate constants (K^0) compared to the aqueous electrolyte (see Supporting Information).

A static membrane-free battery was “assembled” simply by mixing similar volumes of both electrolytes and immersing one carbon electrode in each immiscible phase (at this point, the battery is totally discharged). It is worth to remark that neither physical separator nor ion-exchange membrane was used because catholyte and anolyte are immiscible and spontaneously form two separate phases. This battery was charged to different states of charge (SOC) from 5% to 90% and the potential-current response and current-power relationships were determined in discharge (see Figure S2). Our battery shows very promising behavior especially at 35% of SOC, with an initial discharge voltage of approximately 1.2 V at low currents. This voltage remains above 0.60 V after increasing the current. At this SOC, a power density of 0.6 mW cm^{-2} can be achieved, being similar to those reported in literature for organic RFBs operating with non-aqueous electrolytes^[12,13,41] (see Table S1). Figure 3a shows the charge–discharge profile of our battery and the individual

voltage profiles of each phase when charged to 35% of SOC at low current density. As anticipated by CVs, during the charging stage, in the aqueous catholyte the H_2Q is oxidized to pBQ at a constant voltage of 0.45 V (vs. Ag/AgCl). Meanwhile, the voltage profile of the anolyte displayed the reduction of pBQ to the radical anion (pBQ^-) and to the dianion (pBQ^{2-}). During discharge, the immiscible biphasic system behaves as a common battery with a discharge voltage reaching a plateau at 0.8 V demonstrating the practical feasibility of our Membrane-Free system. The coulombic efficiency of this battery was close to 100% demonstrating that this first example of a Membrane-Free battery, although far from being optimized, already behaves similar to common RFBs employing expensive ion-exchange membranes.^[12] As expected, the ionic liquid anolyte (green curve in Figure 3a) contributes with a larger polarization to the battery overpotential due to its higher viscosity, lower ionic conductivity, smaller diffusion coefficients and slower kinetics of the active species in comparison with aqueous catholyte. Remarkably, during the OCV step the voltage drop at the interphase, which is one of the key issues of this innovative concept, was found to be negligible revealing the high mobility of charge carriers, probably protons, through the interphase. Those results are corroborated in the Figure 3b that shows the polarization curve of the battery. The catholyte potential decreases very slightly from 0.4 V to 0.3 V while the anolyte suffers from higher polarizations, from -0.69 V to -0.25 V with increasing currents. Interestingly, the overpotential across the interphase, is constant and very low which illustrates its stability and its minor contribution to the total resistance of the battery (about 2%). Figure 3c displays the full discharging behavior of our battery at different current densities (voltage cut-off 0.3 V). The membrane-free battery exhibits a constant plateau at about 0.8 V and discharge capacity close to 70% of its theoretical capacity, when discharged at low current densities. Similar to any other type of battery, increasing discharge currents leads to lower capacities due to higher overpotentials, especially in the anolyte. The reversibility of our battery was investigated through deep charge-discharge cycles (from 35% to 0% SOC). During the first 10 cycles, the voltage of the battery was constant and only a minor decrease in capacity was observed probably due to the crossover of active species (Figure S3a). After 20 cycles a reduction in battery voltage caused by the increasing overpotential of the anolyte, was observed. Figure S3b shows that the capacity retention remains above 50% after 30 cycles, confirming the reversibility of our battery.

Before analyzing the origin of battery fading, we assembled a similar battery but employing more concentrated redox electrolytes; 0.1 M H_2Q in 0.1 M HCl for the catholyte and 0.1 M pBQ in $\text{PYR}_{14}\text{TFSI}$ for the anolyte. The higher concentration of the active species causes an improvement in the discharge capacity reaching 90% of the theoretical one at the lowest current density (see Figure S3a). The polarization curve of this battery (see Figure S3a) shows a slightly higher initial discharge voltage than the diluted example (1.4 V vs. 1.2 V), a linear voltage/current relationship and a power density close to 0.6 mW cm^{-2} , similar to the example with diluted electrolytes. Figure S4b shows the discharge profile of the concen-

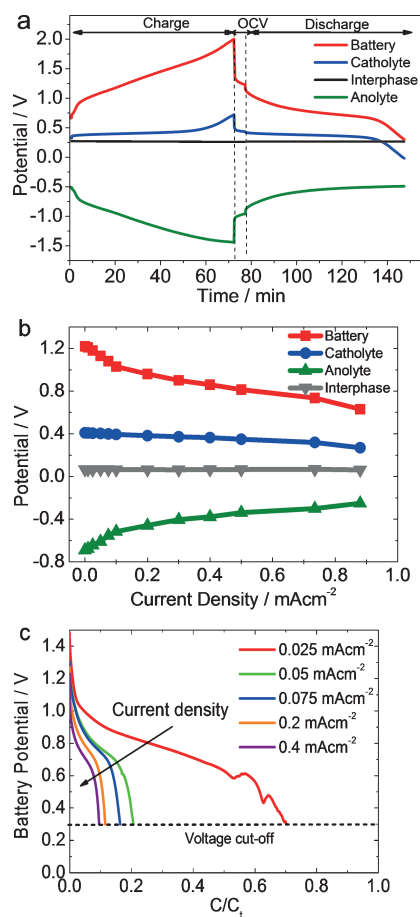


Figure 3. Electrochemical characterization of the membrane-free battery at 35% SOC. Composition of the electrolytes: anolyte; 20 mM pBQ in $\text{PYR}_{14}\text{TFSI}$ and catholyte; 20 mM H_2Q in 0.1 M HCl. a) Charge–discharge experiments at $\pm 0.05 \text{ mAcm}^{-2}$ with a short OCV period. b) Polarization test. c) Discharge profiles of the membrane-free battery at different current densities.

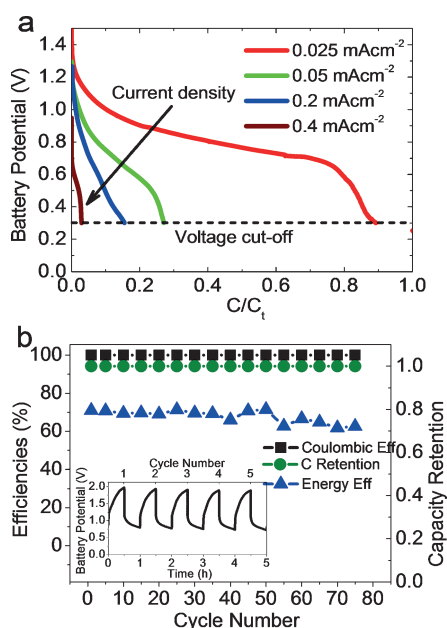


Figure 4. Electrochemical characterization of the membrane-free battery at 35% SOC. Composition of the electrolytes: anolyte; 0.1 m pBQ in $\text{PYR}_{14}\text{TFSI}$ and catholyte; 0.1 m H_2Q in 0.1 m HCl. a) Discharge profiles of the membrane-free battery at different current densities. b) Cyclability study at $\pm 0.2 \text{ mA cm}^{-2}$. Coulombic efficiency, energy efficiency, and capacity retention versus cycles. Inset: Voltage profile of the battery for the first 5 cycles.

trated battery with a discharge voltage plateau of 0.9 V and the individual profiles of each electrolyte and the interphase exhibiting very stable profiles during 8 h. In order to investigate the long term performance of this new battery concept, the biphasic cell was charged/discharged at $\pm 0.2 \text{ mA cm}^{-2}$ during 75 cycles. Under these experimental conditions in which short cycles were employed (low capacitive utilization) the crossover of active species was probably minimized. Figure 4b shows the excellent capacity retention of the system that operates with coulombic efficiencies (CE) exceeding 99% along cycling and with energy efficiencies (EE) of about 70% (the energy efficiency (EE) was calculated as; coulombic efficiency (CE) \times voltage efficiency (VE)). This behavior compares very positively with other organic redox flow batteries reported in literature (see Table S1), confirming the excellent performance of the battery over cycling.

The substitution of the ion-selective membrane by a liquid/liquid interphase raises many questions that makes this simple battery concept very intriguing and fascinating. One interesting issue is related to the crossover of active species through the interphase which is governed by equilibrium thermodynamics through partition coefficients. Although the exhaustive investigation of crossover is out of the scope of this work, CVs of each phase were performed before and after cycling in order to shed light on the changes experienced by the electrolytes (Figure S5a,b). CV curves of catholyte present similar shape but lower peak currents after cycling. This is probably due to crossover of active species (H_2Q or pBQ) from the catholyte to the anolyte. The CV of

the anolyte (Figure S5b) shows a new peak at positive potentials attributed to the redox reaction of H_2Q in ionic liquid.^[34] This demonstrates the crossover of H_2Q from the catholyte to the anolyte. The CV at negative potentials shows higher peak currents after cycling, confirming the crossover of pBQ from the catholyte. Interestingly, the redox peaks were shifted towards more positive potentials probably due to the presence of protons that most likely act as the charge carriers and lead to different reaction pathways (Figures S5c,d). The evolution of redox peaks to more positive potential will lead to lower battery OCV as confirmed during cycling in Figure S3. It should be highlighted that, in this specific example of membrane-free battery in which pBQ and H_2Q represent different oxidation states of the same redox-active molecule, the migration of the species through the interphase does not cause irreversible electrolyte contamination but only a certain capacity loss due to electrolyte imbalance. This imbalance explains the origin of the battery failure at the end of the discharge. As shown in Figure 3a and Figure S4b, the drop of the battery voltage is triggered by the catholyte probably due to the depletion of active species that migrate to the anolyte.

The results reported herein demonstrate the feasibility of this innovative membrane-free battery concept, which relies on immiscible redox electrolytes. The electrochemical performance of this battery does not significantly differ from a conventional one since it maintains a stable discharge voltage profile, high capacity, and good reversibility. The theoretical charge capacity of this membrane-free battery is 5.36 Ah L^{-1} and the theoretical energy density is 2.4 Wh L^{-1} , for an estimated operating voltage of 1.2 V. In fact, using saturated electrolytes with approximately 0.7 M of active species in each electrolyte, the energy density becomes as high as 22.5 Wh L^{-1} . It is worth mentioning that this high value, which has been obtained from a proof-of-concept cell that is not optimized in any respect, is already comparable with recent examples of organic RFBs using membranes.^[12] Further improvements in energy density may be realized by increasing organic molecules solubility and enhancing cell voltages via molecular design and electrolyte choice. Although the concept has been validated for one biphasic system in particular, this technology is very versatile and can be applied to other pairs of redox molecules and immiscible solvents. Moreover, an optimized engineering design with minimum separation between electrodes will decrease the internal resistances dramatically, boosting the performance of the battery. Besides engineering optimization, a judicious selection of immiscible electrolytes containing redox couples in high concentration, with optimum partition coefficients and exhibiting widely separated redox potentials will trigger the development of durable membrane-free batteries with much higher energy and power densities. This concept paves the way for a new battery technology since it considers some physicochemical and thermodynamic aspects never before contemplated in energy storage. New thermodynamic, fluid-dynamic and engineering aspects might become key players in the development of this technology that is not restricted to flowing systems.

Acknowledgements

MFreeB project has received funding from the European Research Council (ERC) under the European Union's Horizon 2020 research and innovation programme (grant agreement No. 726217). The results reflect only the authors' view and the Agency is not responsible for any use that may be made of the information they contain. We also gratefully acknowledge financial support from the Spanish Government through projects ENE2012-31516 and MAT2015-64167-C2-1-R (MINECO/FEDER, UE). P.N. acknowledges the Spanish Government for the personnel grant through the "FPI" program.

Conflict of interest

The authors declare no conflict of interest.

Keywords: electrochemistry · immiscible electrolytes · membrane-free battery · quinones · redox-flow battery

How to cite: *Angew. Chem. Int. Ed.* **2017**, *56*, 12460–12465
Angew. Chem. **2017**, *129*, 12634–12639

-
- [1] J. Rugolo, M. J. Aziz, *Energy Environ. Sci.* **2012**, *5*, 7151.
 [2] Z. Yang, J. Zhang, M. C. W. Kintner-meyer, X. Lu, D. Choi, J. P. Lemmon, *Chem. Rev.* **2011**, *111*, 3577.
 [3] G. L. Soloveichik, *Chem. Rev.* **2015**, *115*, 11533.
 [4] P. Leung, X. Li, C. P. de León, L. Berlouis, C. T. J. Low, F. C. Walsh, *RSC Adv.* **2012**, *2*, 10125.
 [5] M. Skyllas-Kazacos, M. Rychcik, R. G. Robins, A. G. Fane, *J. Electrochem. Soc.* **1986**, *133*, 1057.
 [6] M. Park, J. Ryu, W. Wang, J. Cho, *Nat. Rev. Mater.* **2016**, *2*, 16080.
 [7] J. Winsberg, T. Hagemann, T. Janoschka, M. D. Hager, U. S. Schubert, *Angew. Chem. Int. Ed.* **2017**, *56*, 686; *Angew. Chem.* **2017**, *129*, 702.
 [8] B. Yang, L. Hooper-Burkhardt, F. Wang, G. K. Surya Prakash, S. R. Narayanan, *J. Electrochem. Soc.* **2014**, *161*, A1371.
 [9] K. Lin, Q. Chen, M. R. Gerhardt, L. Tong, S. B. Kim, L. Eisenach, A. W. Valle, D. Hardee, R. G. Gordon, M. J. Aziz, et al., *Science* **2015**, *349*, 1529.
 [10] R. M. Darling, K. G. Gallagher, J. A. Kowalski, S. Ha, F. R. Brushett, *Energy Environ. Sci.* **2014**, *7*, 3459.
 [11] A. Ejjigu, P. A. Greatorex-Davies, D. A. Walsh, *Electrochem. Commun.* **2015**, *54*, 55.
 [12] F. R. Brushett, J. T. Vaughney, A. N. Jansen, *Adv. Energy Mater.* **2012**, *2*, 1390.
 [13] Z. Li, S. Li, S. Liu, K. Huang, D. Fang, F. Wang, S. Peng, *Electrochem. Solid-State Lett.* **2011**, *14*, A171.
 [14] S. K. Park, J. Shim, J. Yang, K. H. Shin, C. S. Jin, B. S. Lee, Y. S. Lee, J. D. Jeon, *Electrochem. Commun.* **2015**, *59*, 68.
 [15] X. Wei, W. Duan, J. Huang, L. Zhang, B. Li, D. Reed, W. Xu, V. Sprenkle, W. Wang, *ACS Energy Lett.* **2016**, *1*, 705.
 [16] T. Liu, X. Wei, Z. Nie, V. Sprenkle, W. Wang, *Adv. Energy Mater.* **2016**, *6*, 1501449.
 [17] X. Wei, W. Xu, J. Huang, L. Zhang, E. Walter, C. Lawrence, M. Vijayakumar, W. A. Henderson, T. Liu, L. Cosimbescu, et al., *Angew. Chem. Int. Ed.* **2015**, *54*, 8684; *Angew. Chem.* **2015**, *127*, 8808.
 [18] T. Janoschka, N. Martin, M. D. Hager, U. S. Schubert, *Angew. Chem. Int. Ed.* **2016**, *55*, 14427; *Angew. Chem.* **2016**, *128*, 14639.
 [19] W. Wang, V. Sprenkle, *Nat. Chem.* **2016**, *8*, 204.
 [20] P. K. Leung, T. Martin, A. A. Shah, M. R. Mohamed, M. A. Anderson, J. Palma, *J. Power Sources* **2017**, *341*, 36.
 [21] P. K. Leung, T. Martin, A. A. Shah, M. A. Anderson, J. Palma, *Chem. Commun.* **2016**, *52*, 14270.
 [22] Y. Xu, Y. Wen, J. Cheng, G. Cao, Y. Yang, *Electrochem. Commun.* **2009**, *11*, 1422.
 [23] Y. Yanga, G. Zhengb, Y. Cuia, *Energy Environ. Sci.* **2013**, *6*, 1552.
 [24] Y. Ding, G. Yu, *Angew. Chem. Int. Ed.* **2016**, *55*, 4772; *Angew. Chem.* **2016**, *128*, 4850.
 [25] V. Viswanathan, A. Crawford, D. Stephenson, S. Kim, W. Wang, B. Li, G. Coffey, E. Thomsen, G. Graff, P. Balducci, et al., *J. Power Sources* **2014**, *247*, 1040.
 [26] L. Joerissen, J. Garche, C. Fabjan, G. Tomazic, *J. Power Sources* **2004**, *127*, 98.
 [27] M. Moore, J. Watson, T. A. Zawodzinski, Jr., M. Zhang, R. M. Counce, *ECS Trans.* **2012**, *41*, 1.
 [28] T. Janoschka, N. Martin, U. Martin, C. Friebe, S. Morgenstern, H. Hiller, M. D. Hager, U. S. Schubert, *Nature* **2015**, *527*, 78.
 [29] W. A. Braff, M. Z. Bazant, C. R. Buie, *Nat. Commun.* **2013**, *4*, 2346.
 [30] R. Ferrigno, A. D. Stroock, T. D. Clark, M. Mayer, G. M. Whitesides, *J. Am. Chem. Soc.* **2002**, *124*, 12930.
 [31] E. Kjeang, R. Michel, D. A. Harrington, N. Djilali, D. Sinton, *J. Am. Chem. Soc.* **2008**, *130*, 4000.
 [32] J. W. Lee, M.-A. Goulet, E. Kjeang, *Lab Chip* **2013**, *13*, 2504.
 [33] C. S. Sevov, R. E. M. Brooner, E. Chénard, R. S. Assary, J. S. Moore, J. Rodríguez-López, M. S. Sanford, *J. Am. Chem. Soc.* **2015**, *137*, 14465.
 [34] M. A. Bhat, *Electrochim. Acta* **2012**, *81*, 275.
 [35] P. S. Guin, S. Das, P. C. Mandal, *Int. J. Electrochem.* **2011**, *2011*, 816202.
 [36] R. A. Potash, J. R. McKone, S. Conte, H. D. Abruña, *J. Electrochem. Soc.* **2016**, *163*, A338.
 [37] W. Duan, R. S. Vemuri, J. D. Milshtein, S. Laramie, R. D. Dmello, J. Huang, L. Zhang, D. Hu, M. Vijayakumar, W. Wang, et al., *J. Mater. Chem. A* **2016**, *4*, 5448.
 [38] J. Carretero-González, E. Castillo-Martínez, M. Armand, *Energy Environ. Sci.* **2016**, *9*, 3521.
 [39] B. Huskinson, M. P. Marshak, C. Suh, S. Er, M. R. Gerhardt, C. J. Galvin, X. Chen, A. Aspuru-Guzik, R. G. Gordon, M. J. Aziz, *Nature* **2014**, *505*, 195.
 [40] M. Galiński, A. Lewandowski, I. Stępiak, *Electrochim. Acta* **2006**, *51*, 5567.
 [41] A. P. Kaur, N. E. Holubowitch, S. Ergun, C. F. Elliott, S. A. Odom, *Energy Technol.* **2015**, *3*, 476.

Manuscript received: April 26, 2017

Accepted manuscript online: June 28, 2017

Version of record online: July 19, 2017